Combined Wind Tunnel Tests and Flow Simulations for Light Aircraft Performance Prediction

Sylvain Mouton, Eric Rantet, Guillaume Gouverneur, Christophe Verbeke

47th International Symposium of Applied Aerodynamics
Paris, 26-28 March 2012

FP23-2012-MOUTON

COMBINED WIND TUNNEL TESTS AND FLOW SIMULATIONS FOR LIGHT AIRCRAFT PERFORMANCE PREDICTION

Sylvain Mouton [(1)], Eric Rantet [(2)], Guillaume Gouverneur [(3)], Christophe Verbeke [(4)]

[(1)] ONERA – the French Aerospace Lab – F-59045 Lille, France, sylvain.mouton@ONERA.fr
[(2)] Aviation Design, 38 ZI Le Chenet – 91490 Milly-la-Forêt, France, aviation.design@wanadoo.fr
[(3)] ESTACA Graduate, former ONERA intern, guillaume.gouverneur@estaca.fr
[(4)] ONERA – the French Aerospace Lab – F-59045 Lille, France, christophe.verbeke@onera.fr

ABSTRACT
This paper presents an example of the use of ONERA L2 wind tunnel, complemented by CFD computations, to derive a complete set of aerodynamic characteristics on a low-speed light aircraft configuration.

1. INTRODUCTION

In the past decade, evolving regulation and technical progress have favoured renewal on the market of very light to light aircrafts. In the same time, the demand for small tactical Unmanned Aerial Vehicles (UAV) has also considerably grown. Contrary to large aircraft manufacturers who benefit from decades of experience and skilled teams, many light aircraft and UAV manufacturers have limited resources to invest into the creation of aerodynamic and flight dynamic teams. As a consequence, they are confronted to difficulties with the accurate determination of the aerodynamic characteristics of their products.
Indeed, although it is a critical set of data in the determination of performance criteria such as range, endurance, rate of climb, stability or control efficiency, the aerodynamic characteristics of a complete aircraft over its whole flight domain are still difficult to determine accurately and to optimise. This determination may rely on three different tools: CFD, flying model and wind tunnel tests.
Numerical simulation with CFD software is a very interesting tool for aerodynamic design. However, it is still both expensive and not fully reliable, because of the cost of the major licensed software, of the required computational power, of the level of expertise to properly run and interpret results, and of physical hypotheses on turbulence modelling.
A second possibility is to use a flying reduced-scale model of the aircraft, and attempt to derive some characteristics of the full scale aircraft from data measured during remotely-controlled flights. Experience tend to prove that it is very difficult to get quantitative measurements from such experiments and even more difficult to extrapolate them to the behaviour of the full scale aircraft.
A third possibility, historically the most used [1], is to perform wind-tunnel tests. Unfortunately, major wind tunnels are large facilities that tend to specialise in highly accurate test campaigns, devoted to the sharp optimisation of large transport aircrafts, therefore expensive and not well suited to smaller business plans. Smaller wind tunnels, often operated by universities, can only offer small test sections, which constrain to the use of very small scale model, difficult to manufacture with suitable accuracy and to equip with measurement devices.
As an example of solution brought to this problem, this paper presents the use of ONERA L2 wind tunnel combined with CFD computations to derive the aerodynamic characteristics of the Eole unmanned aircraft.

2. THE L2 LOW-SPEED LARGE-SIZE WIND TUNNEL

2.1. Wind tunnel circuit

The ONERA L2 wind-tunnel located in Lille was put into service in 1968, enlarged and completely renovated in 2002 and continuously upgraded ever since. It has been mostly used to investigate the flow field around ships, trains, buildings and for numerous industrial applications, including the prediction of wind forces on ground structure, pedestrian comfort, etc. In an attempt to bring an answer to a light aircraft manufacturer, it was

used for aeronautical testing for the first time in 2009.

The ONERA L2 facility is an open-circuit wind-tunnel offering a large test section: 6.5 m wide × 2.5 m high × 10 m long. It is located in a closed shed of large dimensions (725 m^2) to allow free return of the flow. The flow is driven by 18 electric engines, individually controlled, for a total power of 125 kW. It operates at ambient temperature and pressure. Velocity is continuously adjustable up to 19 m/s, such a low speed being a counterpart of the large test section size and limited power. However, the Reynolds number is still 0.43 million at 19 m/s based on $1/10^{th}$ of the square root of the test section area ($0.1\sqrt{15}$ = 0.387 m).

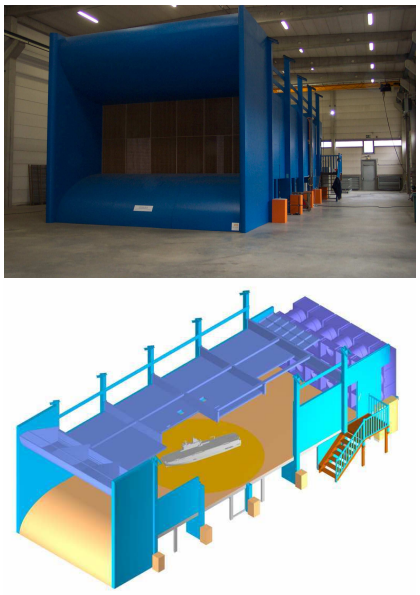

Figure 1: The L2 wind-tunnel, photograph (top) and 3D view (bottom)

The flow enters the test section through a 2D convergent with a 2.2 contraction ratio. Honeycomb panels with cells of 5 × 5 × 30 cm are used at the end of the convergent to line up the flow field in axial direction. These panels can be fitted with a grid of cylinders non-uniformly distributed between the floor and roof of the tunnel in order to generate a flow velocity profile reproducing the marine boundary layer. This device is used during test of ground structures or ships. Downstream of the test section, a small diverging section leads to the 18 fans. The flow passage also ensures the cooling of the electric engines driving the fans. The flow is then vented to the rear part of the shed where it is allowed to freely diffuse to the side and top of the test section, where it returns to the entrance of the tunnel with a slow velocity. No cooling device is used to hold the temperature of the flow constant, but natural heat conduction keeps the rise in temperature limited to about 5°C per hour of continuous operation. Air extraction and destratification can also be used to remove fumes and tracers used with some measurement techniques. A heating system is available for winter operations. The wind-tunnel is mainly built with stratified wood panels screwed on wooden frames, painted in dark blue or grey with markers to ease flow visualisation.

2.2. Wind-tunnel operation

The wind tunnel is operated from an air-conditioned, soundproof control room located right in front of the test section. It is designed to be run by a single operator, monitoring both the wind-tunnel flow, data acquisition, and performing the requested configuration changes on the model. Five webcams are used to monitor operations in and around the test section.

Access to the test section is provided by a 135 × 205 cm door and a stairway. Access to the shed is possible with a vehicle through a 4.35 × 4.60 m door. An 8-bar compressed air network is available, as well as water supply. A small workshop is located in the underground of the wind tunnel shed for minor intervention on the model. Heavier machining operation can be carried out on request by specialised model manufacturing team on site. Access to the wind-tunnel building is restricted to authorized personal and controlled by electronic access card door. The ONERA site is protected 7/7 24/24. Visiting customers can be provided with an office and internet access.

2.3. Flow quality

The flow inside the test section is known to be significantly turbulent, which presents some drawbacks such as model vibrations, but helps triggering boundary layer transition. The turbulence characteristics are well documented for tests with the grid generating marine boundary layer [4], but still need to be determined without this grid. A mean flow downwash of 0.2° in the centre of the test section was measured, probably caused by the asymmetry of the free-return flow path. It is also known that the boundary layer on lateral walls is very thick and one should avoid placing model in this area. The test section presents no divergence to compensate for the growth of the wall boundary layer, which results in a measured static pressure gradient of 7‰ of dynamic pressure per meter in streamwise direction.

2.4. Model mounting

For marine and ground structures or vehicles, the model is mounted on the tunnel floor, using a balance if force measurement is requested. The middle part of tunnel floor is equipped with a Ø6 m plateau rotating over 360° to perform test under for all wind directions.
For aeronautical testing, the model may be hold from below with a mast, or from the rear with a sting. Several supports are available off the shelf, such as a Ø40 mm mast and a cranked mast for rear mounting (Figure 2).

Figure 2: Eole model in L2 wind tunnel

The attitude of the model in the tunnel is controlled thanks to a carriage travelling onto a hemicylindrical cradle. This allows the model to rotate around the wind tunnel centre without translation. A 40° range in angle of attack is permitted by this system. Rotation of the mast around its axis allows a 360° range for sideslip angle, although usual tests are limited to ±20°. The whole system is remotely controlled to perform fixed point or continuous polar measurement at a velocity up to 0.3°/s.

2.5. Measurement techniques

A wide range of measurement techniques can be used in the tunnel, most of them being facilitated by the easy access to the model, and its large size. Thanks to the low velocity and the width of the tunnel, operators can stand in the test section during runs to manipulate, observe and record pictures or measurements.
The Lille centre is equipped with a metrological laboratory to perform in-house sensor calibration. ONERA is certified ISO 9001:2008 for orienting and performing research work for aerospace and defence.

2.5.1. Qualitative flow visualisation techniques

Qualitative flow visualisation techniques are very useful for a quick assessment of flow pattern. The main visualisation techniques used in L2 wind-tunnel are laser tomoscopy, oil flow and wool tufts. Pictures and videos are recorded with professional HD cameras.
Laser tomoscopy is performed using a YAG 5W laser connected with an optic fibre to a laser sheet generator. The laser sheet can be easily hooked to the roof of the test section or any available support and manually or remotely oriented towards the region of interest. An oil/water fume generator is used to seed to flow. It is generally operated by hand, the operator being positioned somewhere upstream or on the side of the model, far enough to minimize flow distortion.
Oil flow is used to observe skin friction pattern. Because of the low dynamic pressure, a use of low viscosity oil is made necessary and it is preferably used on nearly horizontal surfaces to avoid gravity effects. Linseed or synthetic oils with white titanium oxide pigments are generally used.
Wool tufts are used to identify local flow direction and have been used to understand stall mechanisms on wings (see Figure 12 in the end of this paper).

2.5.2. Force and pressure measurements

Forces on the model or part of the model are measured thanks to aerodynamic balances, either internal or wall mounted. The balances used are borrowed from the ONERA balance extensive collection. They are calibrated and checked by a specialised team in Modane. Uncertainty of the balance measurement is generally better than 10^{-3} of the measurement range.
Pressure measurements are carried out thanks to a PSI® 8400 system, and up to three modules of 32 channels with ±2 500 Pa measurement range (ESP32), which yield to an absolute uncertainty of ±0.02 in pressure coefficient. Better relative accuracy (from one pressure tap to another during the same measurement) can however be obtained (see e.g. Figure 3). The wind-tunnel is also permanently equipped with an absolute atmospheric pressure probe, and an independent DRUCK® differential pressure sensor connected to the main Pitot tube to backup PSI® measurements of the dynamic pressure.

2.5.3. Volume measurements

Exploration of the flow-field around the model is made easier by a traverse system located in the downstream part of the test section. This system is a 3-degree-of-freedom remotely controlled metallic frame, enabling access to most parts of the volume of the test section. Alternatively,

measurement devices can easily be screwed on the wooden walls or floor of the tunnel.
Measurements have been carried out with hot wire anemometry, with Prandtl tubes and with 5-hole probes. CO_2 concentration can also be measured when this gas is used as a tracer in pollutants, or plume dispersion for example.
2-component and 3-component PIV technique has also been used for detailed insight of the flow field structure [5]. Optical access to the test section is provided by some removable transparent panels on the roof and lateral wall. However, as previously mentioned it might be easier to install the camera within the test section if the flow perturbation is considered acceptable. A team of PIV specialists with in house software and a broad experience is available on site to carry out the measurements.

2.5.4. Data acquisition system

Apart from the standalone PSI® pressure measurement system, the instrumentation of the wind tunnel is built around type B VXI mainframe and filters. The VXI mainframe integrates a command module based on an IEEE 1394 interface, a 32-channel relay card E1463, a DSP module E1433, and an arbitrary source generator E1434. Signal is conditioned using “sister cards” SCP of different types. A 64-channel VT1422A card is used to acquire most measurements, including voltages of balance strain gauges, inclinometers signal, etc. with a maximum sampling frequency of 25 thousand samples per second. It is used over a ±10 V range. Voltages are converted on 16 bits; therefore voltage resolution is about 0.3 mV.

2.6. Data reduction and corrections

The dynamic pressure in the wind tunnel is measured by a central Prandtl tube located 2 m downstream of the honeycomb. Tunnel calibration was performed to relate the dynamic pressure at this location to the dynamic pressure in the tunnel centre. The temperature, atmospheric pressure and moisture level in the wind-tunnel building is measured in real time during tests, which allows density determination, and then velocity, Mach and Reynolds numbers, assuming a constant density flow.
Recorded data are most of the time reduced to non-dimensional coefficients to ease interpretation. Corrections to the measurements may include dead weight subtraction, cavity corrections, buoyancy correction, wall and support correction, depending on test configuration and requests. Wall and support corrections are computed using simplified potential flow modelling, solved thanks to a singularity distribution [1], and checked using pressure measurement on the wind tunnel walls (Figure 3).

3. A TYPICAL MODEL: THE EOLE AIRCRAFT

3.1. Context of the Eole project

The goal of this project is to build a small-scale demonstrator to investigate feasibility of airborne rocket launching, i.e. a way to launch rockets from an aircraft in altitude rather than from ground installations. Such an idea presents a number of advantages that will not be discussed here. The Eole project is led by ONERA under a contract of the CNES (French National Centre for Space). The CNES is supporting several technological demonstrators for future launch projects. In the framework of the Perseus programme (*Projet Etudiant de Recherche Spatiale Européen Universitaire et Scientifique*) those projects involve students in scientific activities.
The envisaged demonstrator should demonstrate ability to automatically carry and release a rocket in altitude, before the rocket ignites and takes appropriate ascending trajectory, but without actually putting a satellite into orbit. In order to achieve this goal, a size of about 6.7 m span for 200 kg MTOW was selected. The general patent-pending architecture is dictated by the specific mission. The Eole wind tunnel campaign used a 1/2.3 scale model of this demonstrator, with a generic rocket shape.

3.2. Model design and main characteristics

The model was designed and manufactured by Aviation Design, a SME with long years of experience in R&D, CAD and rapid prototyping for the aerospace industry as a subcontractor for major aerospace companies such as Dassault Aviation, Thales, CNES and ONERA on civilian and military research projects. Aviation Design has a large experience in the design and manufacture of UAVs and wind tunnel models for the aeronautic industry. It also designs and builds mechanical and electronical assemblies, and employs specialists in high tech composite parts, mainly dedicated to research programs. Its small structure allows fast reactivity, process decision, and rapid prototyping process. Aviation Design was founded in 1993 and is located in Milly-la-Forêt (Essonne, France).
Regarding this project, previous experience of wind tunnel models and CAD design was a very valuable asset to fulfil the exact requirements at low cost. The model was entirely designed using

Catia® V5 CAD software, which is particularly useful to check the interface requirements with the wind tunnel equipment.
A specification document was issued by ONERA to state the design constraints and demands. A design review was organised to make sure the mounting of the model in the wind tunnel would go smoothly. Thanks to the low dynamic pressure during the test, the mechanical resistance of the model is easily verified without a careful dimensioning of critical parts.
The designed model has a span of 2.9 m and a weight of 8.5 kg. It has 10 moveable control surfaces and flaps, the setting of which can be adjusted continuously over their whole range and is controlled by graduated quadrants.

3.3. Model manufacture

The model was built out of composite material in order to minimize its cost and its manufacturing time using fast prototyping method. It should be underlined that this manufacturing technology was made possible by the large size of the model and the low forces to sustain. As an example, a typical tolerance on the airfoil shape of 0.1% of chord [1] translates into a 0.2 mm tolerance in this case. If the model had a span of 70 cm instead of 3 m, the same demand would have led to a 0.05 mm tolerance, beyond the capability of composite material technology.
Negative moulds were CNC machined in hard polyurethane resin. Each model parts, including the control surfaces, required the production of two half moulds to obtain a perfect precision. The model itself was laminated in glass fibre and epoxy resin, using vacuum process. The surface coating and finish is carried out manually. The model was painted in matt black paint to ease flow visualisation during the test. The moulds can be used several times, which has allowed the production of three models of same size, one being used for the wind tunnel tests, one for flight tests and the last one for ground exhibition during the last Paris Air Show.
The complete wind tunnel model was designed, machined and moulded in about 3 months.

3.4. Model measuring equipment

The model is equipped with 60 pressure taps fitted in the composite skin. There are connected to two ESP32 pressure sensors located in the central pod (the fairing in the middle of the wing designed to hold the rocket), thanks to vinyl tubes routed during the manufacture. Here again, the large size of the model made it possible to easily integrate the tubing, the sensors and the balance inside the model.
The attitude of the model is measured thanks to two redundant inclinometers located in the two fuselages. A reference surface is also used to check the model attitude (wind off) with an external inclinometer.
The model was mounted on the support thanks to an internal 6-component balance. 1‰ of the balance measurement range represented a drag coefficient of 0.007, a lift and side force coefficient of 0.03 and moment coefficients between 0.005 and 0.01.

3.5. Test procedure

The wing of the model is designed using an ONERA OAPV15i laminar airfoil. Considering the Reynolds number in the wind tunnel flow, the boundary layer transition was forced on the model by means of 0.5 mm thick zig-zag self-adhesive strips. Preliminary 2D simulations were carried out in order to help selecting a proper position for the strips, with the aim to preserve as much as possible the aerodynamic characteristics of the airfoil at full scale flight Reynolds number. Effectiveness of the transition was experimentally checked by means of oil flow visualisation.

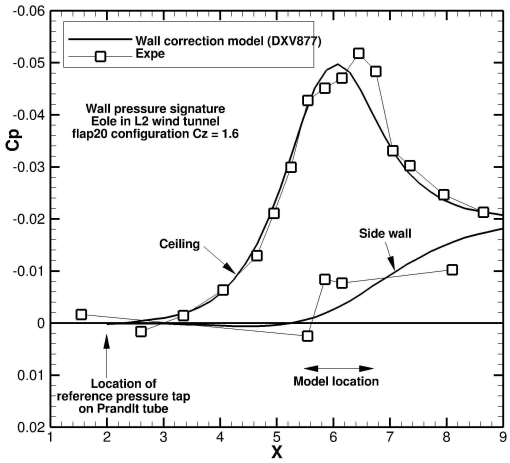

Figure 3: Pressure distribution on wind tunnel walls

All measurements were carried out at fixed sideslip and angle of attack (AoA), and the average of data acquired during measurement time at each fixed point was retained. Usual data reduction and correction mentioned in §2.6 were applied. The Figure 3 shows measured and modelled pressure distribution on the wind tunnel walls, used to check the wall corrections. The acceleration of the flow passing on top of the model is nicely predicted. It especially validates

the wall effect on AoA, which is the most significant wall correction term in that case with value up to 0.5°.
About 100 polars were performed during the wind tunnel campaign. A typical duration of such a campaign, from model reception to model restitution would be about 5 weeks. Actions to increase measurement productivity by reducing polar duration were identified for future tests.

4. COMPLEMENTARY CFD COMPUTATIONS FOR EOLE TESTS

The goals of the CFD computations carried out in the course of this study were twofold: the main objective was to extrapolate the wind-tunnel data to flight conditions in terms of Reynolds number; a secondary objective was to complement the test in the understanding of flow phenomena on the model.

4.1. The CFD model

4.1.1. Meshing technique

The flow simulations on this configuration were carried out on a mesh making use of Chimera technique to ease the integration of the high-lift flaps at different settings. The mesh of the half aircraft depicted in Figure 4 comprises 5.1 millions cells for the clean configuration plus 8.1 millions cells for the flaps. Considering their above mentioned objectives, most simulations were carried out without the nacelles and the rocket to simplify mesh generation. However, as will be explained latter, clean configurations with nacelles were also simulated, with a nacelle part comprising 0.9 million cells. Wall refinement was adjusted to match the requirement of the low-Reynolds turbulence model, i.e. a thickness of the first layer of cells of the order of 1 wall unit. The boundary layer is then discretised by about 30 layers of cells.

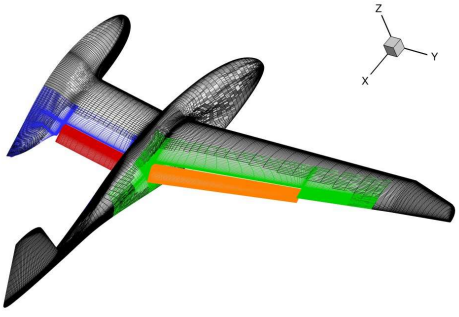

Figure 4: Eole mesh used for CFD computations

4.1.2. Flow solver

The ONERA in-house multi-purpose *elsA* solver [3] was used to solve RANS equations for the flow on this configuration. *elsA* is a structured multiblock flow solver implementing numerous CFD techniques and turbulence models. For this study, the *k-ω* turbulence model of Menter was used, without SST correction. The centred second-order numerical scheme of Jameson was used, with fourth order artificial dissipation, using a coefficient k_4 of 0.032. Choi-Merkle preconditioning method was applied to the convective system to improve numerical accuracy and convergence rate. Pseudo-time marching was realised thanks to a backward Euler scheme. Implicit formulation solved by a LU-SSOR method as well as a one-level multigrid method were also used to speed up convergence. A typical computation took 1 to 5 hours on the ONERA parallel supercomputer.

4.1.3. Boundary conditions

Simulations were carried out for wind tunnel flow conditions and for flow conditions representative of real scale flight, as summarised in Table 1. Non-reflection boundary conditions were used on the far-field boundaries, and adiabatic walls on the aircraft surface
The transition of the boundary layer was modelled in the simulations using the Arnal-Habiballah-Delcourt criterion, complemented by Gleize to properly account for transition trough laminar bubbles

	Wind-tunnel	Flight
Mach number	0.055	0.12
Reynolds number	$0.23\ 10^6$	$1.14\ 10^6$
Transition	forced	natural

Table 1: Flow conditions for CFD simulations

4.2. Validation of simulations

In order to validate the results of the simulations, a comparison is carried out between the wind-tunnel test data and the simulations under wind-tunnel flow conditions. It is reminded that these simulations do not include the nacelles on the inner wing of the model.
An example of such a comparison in terms of pressure distribution on the outer wing is presented in Figure 5. The simulations are in very good agreement with the experimental data for all cases except the 40° flap setting case for which the lift of the main body is slightly overestimated. The plateau pressure level in the massively

separated flow over the flap at 30° and 40° settings is accurately predicted.

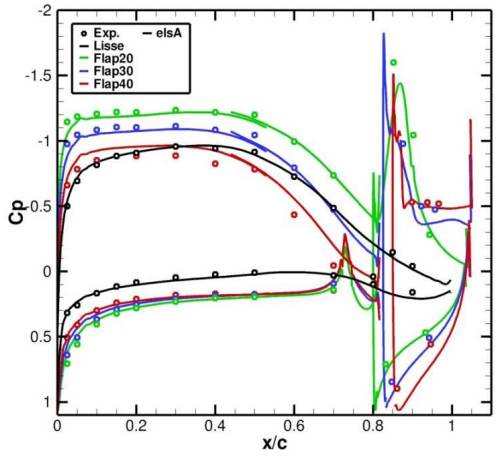

Figure 5: Experimental and simulated pressure distribution on outer wing for different flap settings (AoA = 5°)

Concerning forces (Figure 6), general agreement is fairly satisfactory but maximum lift is over predicted by the computations for most configurations. Pitching moment is accurately predicted. The large discrepancy in drag is caused by the nacelles not being included in the simulations, as will be explained in §5.3.

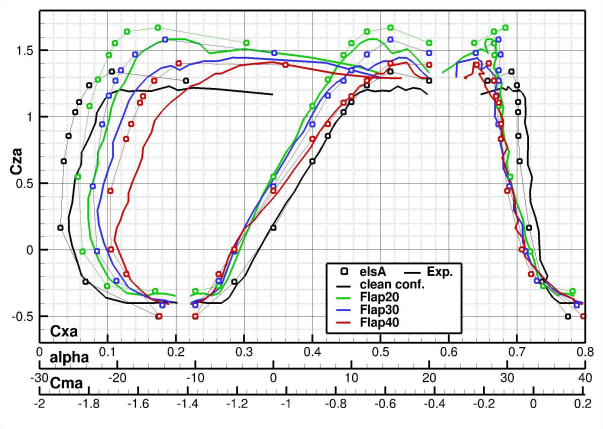

Figure 6: Experimental and simulated force coefficients for different flap settings

4.3. Reynolds number extrapolation

Having performed simulations both for wind-tunnel and flight flow conditions, the difference in force coefficient between those two cases can be identified and applied to the experimental data as a Reynolds extrapolation term. To compute those difference terms, a reduced AoA $\bar{\alpha}$ is first defined by linearly scaling the AoA between positive and negative stall points, as illustrated in Figure 7. The differences between polar curves are then determined at iso reduced AoA, and also applied to the test data at iso reduced AoA. This method allows extrapolation of the lift slope, the maximum lift coefficient and the stall angle, even in case of disagreement between simulations and experiments concerning stall characteristics.

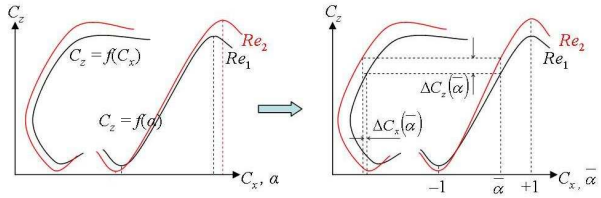

Figure 7: Principle of Reynolds extrapolation

It is however impossible to run CFD simulations for all tested configurations and under all flow conditions. Therefore, the Reynolds extrapolation was determined for the longitudinal coefficients only, deemed the most critical data in terms of flight performance evaluation. No Reynolds effect is evaluated for control surfaces efficiency for example. This was considered a conservative approach since the efficiency of the control surfaces is very likely to increase with Reynolds number, being therefore slightly better in actual flight than predicted in the wind-tunnel. The same holds for lateral coefficients in sideslip.

Reynolds extrapolation yields expected results for a Reynolds effect: the lift slope is increased, as well as maximum lift, while the drag is decreased and the pitching moment is nearly unchanged (Figure 8). The exact magnitude of each effect depends on the flap configuration considered.

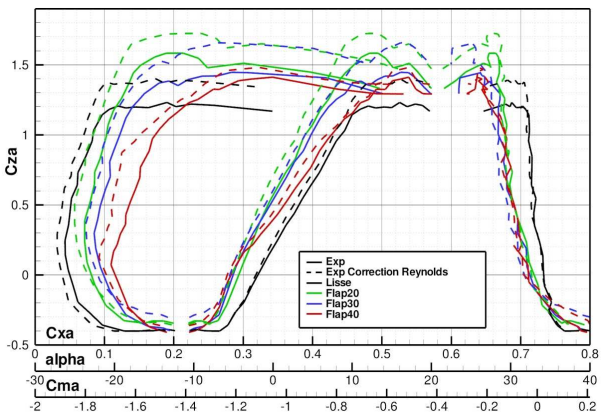

Figure 8: Reynolds extrapolation of wind tunnel test data

5. EXAMPLE OF RESULTS FROM COMBINED WIND-TUNNEL AND CFD DATA

This section gives some examples to illustrate the kind of result obtained from the test campaign

complemented by CFD calculations, and their consequences on the aircraft and the project.

5.1. Main performance data

As previously illustrated in Figure 8, the wind-tunnel tests deliver a full set of longitudinal performance data, for every flap settings. Only a few comments are given here to illustrate the lessons learned from the wind tunnel test. Maximum lift is reached for a flap setting of 20°, to be used for take-off. Larger flap angles are less efficient in generating lift and are rather to be used as airbrakes. Static stability is validated as revealed by the slope of the pitching moment curve. It is augmented by flap deflection. Because of the nacelles flow separation to be discussed in §5.3, the maximum lift-to-drag ratio is only 15, quite disappointing considering the aircraft configuration.
An example of result for a polar in sideslip is provided in Figure 9, along with simulation results using two models of different fidelity (*elsA* RANS solver described in §4.1.2, and a panel code called Tagazou). One of the outcome of the test is that the aircraft is laterally stable, a characteristic also well predicted by the flow simulations. It appears that the rolling moment coefficient does not exactly vanish for zero sideslip, which may reveal a small model dissymmetry or flow non-homogeneity in the test section.

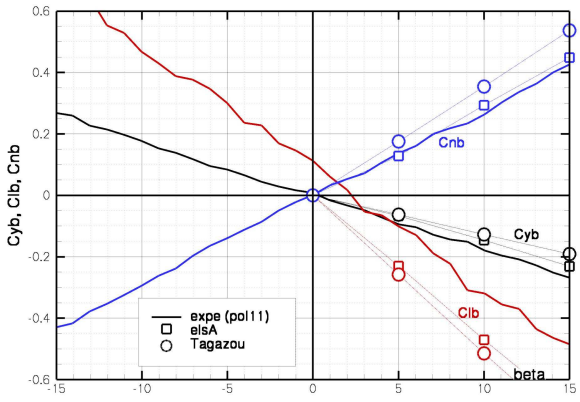

Figure 9: Results from a sideslip polar

5.2. Efficiency of control surfaces

A full database was generated in order to check the efficiency of all control surface over the complete flight envelope, including partial failure cases since this aircraft has 4 ailerons on wings and 2 independent control surfaces on the rear empennages that are used both as elevator and rudder.

As an example of the collected results, the Figure 10 shows the effect on longitudinal force coefficients of the empennages control surfaces used as elevators. The main effect on pitching moment is clearly visible, but the effect on lift and drag is also significant and asymmetric, especially for large deflection angles.

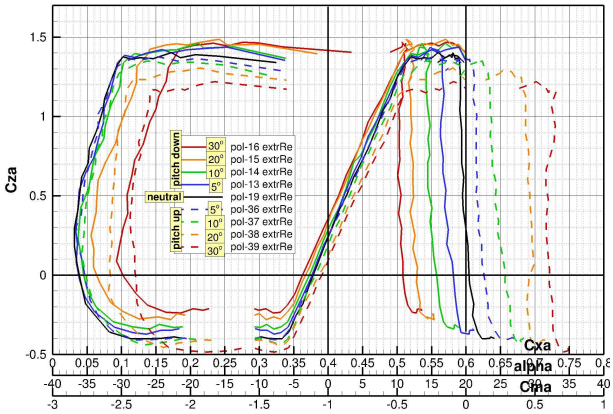

Figure 10: Elevator efficiency

5.3. Effect of the engine nacelles

During the course of the test campaign, undesirable flow separation was located on the nacelles pylons, which was suspected to cause early stall of the inner wing, the large drag discrepancy mentioned in §4.2 and the rather poor lift-to-drag ratio of §5.1. Unfortunately, the wind-tunnel model was not constructed to allow dismounting of the nacelles and pylons, so that it was impossible to experimentally check their effect. To provide a better insight on that point, simulations of the clean configurations with nacelles were carried out.

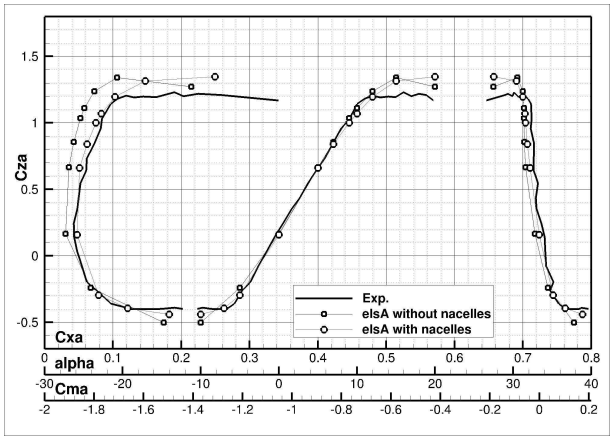

Figure 11: Simulations of nacelle effect on performance

Some results are presented in Figure 11. It can be seen that the nacelles have indeed a very

significant impact on drag, and that the simulations with nacelles are in good agreement with the test results. On the opposite, in spite of their effect on inner wing flow separation, they have little effect on lift and stability. Qualitative comparison of the surface flow topology also gives convincing results, as illustrated in Figure 12.

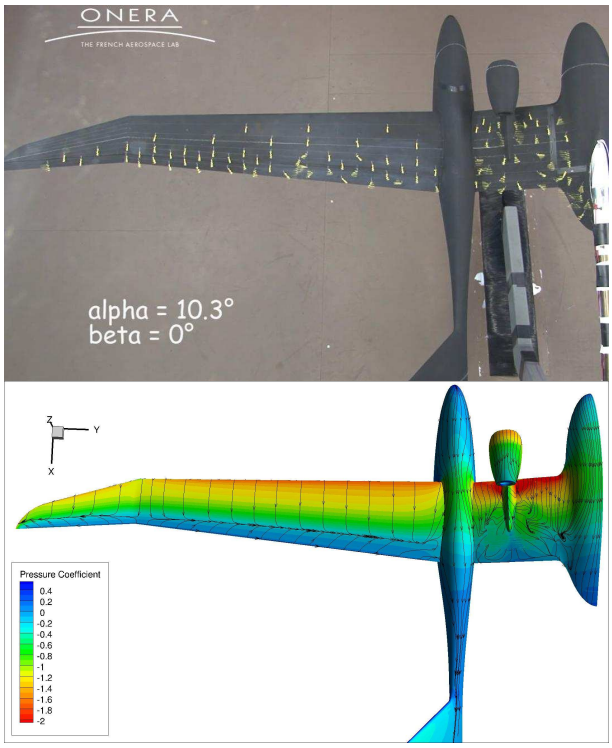

Figure 12: Stall onset visualised by wool tufts (top) and simulated by CFD (bottom)

From obtained results, it can be evaluated that the lift to drag ratio would be about 21 instead of 15 without nacelles. As a consequence of these findings, the nacelles and pylons are going to be redesigned in the course of the ongoing Eole project.

6. CONCLUSION

This paper presented a solution available at ONERA to derive the aerodynamic characteristics of a light aircraft or UAV. This solution is widely based on the L2 low-speed wind-tunnel, which can accommodate large-size models, up to 3.5 m span. The Eole test campaign was used as an example throughout the paper. The collected database is being exploited in the ongoing Eole project to design the aircraft control laws, to develop a training flight simulator, to predict performances and to perform safety analyses supporting the official request for flight authorisation.

It was illustrated that large size models present numbers of advantages over smaller ones, in terms of technology, manufacture, measuring equipment and cost effectiveness. As a result, and although it is counter intuitive, the cost of a large model is much less that the cost of a smaller one for comparable accuracy and test capabilities. Small tactical UAVs could even be tested at full scale in the wind tunnel.
The wind-tunnel tests are complemented by CFD simulations to provide Reynolds extrapolation and better flow understanding. The ONERA solver *elsA* is used to serve that purpose.
Although the L2 wind-tunnel cannot claim for comparable level of accuracy and productivity as larger industrial low-speed wind-tunnels such as ONERA F1, it is regarded as a versatile facility that has successfully provided valuable results on numerous industrial applications including aeronautical ones in the past years. The wind tunnel facility and operation procedures are still being continuously improved in the fields of performance, flow quality, productivity and measurement techniques.

7. REFERENCES

1. Pankhurst, R.C., Holder, D. (1952). *Wind-Tunnel Technique.* Sir Isaac Pitman & Sons.
2. Vaucheret, X. (1988). Recent Calculation Progress on Wall Interferences in Industrial Wind Tunnels. *La Recherche Aérospatiale*, No. 3, pp 45-47.
3. Cambier, L., Veuillot J.-P. (2008). Status of the elsA CFD Software for Flow Simulation and Multidisciplinary Applications, 26th AIAA Applied Aerodynamics Conference, AIAA 2008-664, Reno, January 7-10, 2008.
4. Herry, B. (2010). *Etude aérodynamique d'une double marche descendante 3D appliquée a la sécurisation de l'appontage des hélicoptères sur les frégates.* (*Aerodynamic Study of a Double Backward Facing Step and Application to the Safety of Helicopters Landing on Frigates*) Doctoral Thesis of the Université de Valenciennes et du Hainaut Cambrésis
5. Herry, B., van der Vorst, J. (2010). Towards the impact of flow bi-stability on the launch and recovery of helicopters on ships. AIAA Centennial of Naval Aviation Forum, AIAA 2011-7043, September 21-22, Virginia Beach